J Mater Sci (2008) 43:1180–1190
DOI 10.1007/s10853-007-2301-7

Surface damage of brittle polymer resulting from static cyclic contact loading

Pratip Vongbandit · Tadeusz A. Stolarski

Received: 5 July 2007 / Accepted: 5 November 2007 / Published online: 4 December 2007

Abstract Morphology of damage inflicted on the polymethylmethacrylate (PMMA) plate in static point contact with a ball made of five different materials under cyclic normal load has been presented. It is argued that the counterface material plays an important role in the damage process and the extent of damage inflicted on the PMMA plate.

Introduction

Surface damage inflicted on materials by cyclic contact stress can be classified into two categories: wear and fatigue. Contact failures are produced by quite complex mechanisms and are influenced by numerous parameters such as contact load conditions, surface conditions, material properties and lubrication. In order to understand how these parameters affect surface damage, experiments must be carried out with test conditions carefully controlled.

Ball-on-flat contact is a simple test configuration frequently used to study contact fatigue. Earlier studies on the damage of materials included such contact pairs as steel ball/case hardened steel [1], tungsten carbide ball/silicon nitride [2, 3], tungsten carbide ball/soda-lime glass, porcelain and silicon nitride [4], steel ball/ titanium nitride, molybdenum disulfide and TiN + MoS_2 coatings on steel plate [5].

P. Vongbandit (✉) · T. A. Stolarski
Department of Mechanical Engineering, School of Engineering and Design, Brunel University, Uxbridge, Middlesex UB8 3PH, UK
e-mail: pratip.vongbandit@brunel.ac.uk

A test sample can be damaged in the form of cracks and wear debris produced under oscillating load in the ball-on-flat configuration. Ring cone cracks, radial cracks and lateral cracks are usually produced in brittle or relative brittle materials. The first type of crack generally appears in most cases. This crack originates at the edge of contact where maximum tensile stress is present according to stress calculations by Hertz's theory [6]. The position of this kind of crack depends on load level, and types and properties of materials. In case of hardened steel the ring cone crack is located at or up to 17% outside the contact radius [1]. For homogeneous fine grain polycrystalline alumina ceramic cracks occur outside the contact circle but the damage develops beneath the contact circle in the coarse-grain alumina [7].

In the last decade, damage mechanisms of brittle materials subjected to cyclic contact load have been proposed. Materials with heterogeneous microstructure are damaged at preferential side [3]. Kim et al. [4] demonstrated that two damage modes include tensile driven macroscopic cone cracks and shear driven distributed micro damage accumulation of radial cracks and secondary cone cracks. The former is a brittle mode and the later is a quasi-plastic mode.

A number of researchers [3, 8] have proposed wear mechanisms induced by contact cyclic loading. Wear is found to be most severe in slip area of the contact where shear stress is created due to Young's modulus and Poisson's ratio mismatch between contacting materials during loading and unloading cycles.

A considerable research effort has been devoted to study contact damage of brittle polymers. However, wear process and mechanism of polymethylmethacrylate (PMMA) under static cyclic contact loading has not been substantially elaborated, even though many experiments were carried

out on model contacts such as linear fretting fatigue or torsional fretting fatigue [9, 10].

This article presents results of investigation into the forms of damage of PMMA in static contact with spheres made of a number of different materials under cyclic normal loading. The main motivation for the study presented in this article was to ascertain how and to what extent the counterface material affects the damage morphology of a brittle polymer such as PMMA.

Experimental procedures techniques

Materials

A commercially available PMMA, in the form of a sheet with thickness of 5 mm, was used. Test specimens were cut out as rectangular plates with length of 25 mm and width of 10 mm and surface finish as supplied. Spheres with diameter of 12.7 mm made of silicon nitride, steel, bronze, aluminium and PMMA were used as counterfaces. Prior to testing, the balls, except PMMA ball, were thoroughly cleaned with general purpose solvent. PMMA ball was cleaned using soap. Mechanical properties of the balls and PMMA plate are listed in Table 1.

Test apparatus

A ball-on-flat contact configuration was created in the specially designed test rig shown schematically in Fig. 1. An eccentric shaft (1), connected to and driven by an electric motor, generates oscillatory movement of the slider (3) via the loading arm (2). This results in cyclic compression of the spring (4), which in turn imposes cyclic loading on the ball and the test plate (7) via slider (5). The apparatus is capable of generating a constant sinusoidal load pattern, where amplitude and mean values can be adjusted.

Table 1 Properties of materials using in this study

Materials	Young's modulus (GPa)	Poisson's ratio	Tensile strength (MPa)
PMMA plate	3.3	0.37	80
Silicon nitride ball	315.0	0.27	524
Steel ball	207.0	0.30	>2145
Aluminium ball	70.6	0.34	93
Bronze ball	105.0	0.35	265
PMMA ball	2.95	0.30	75

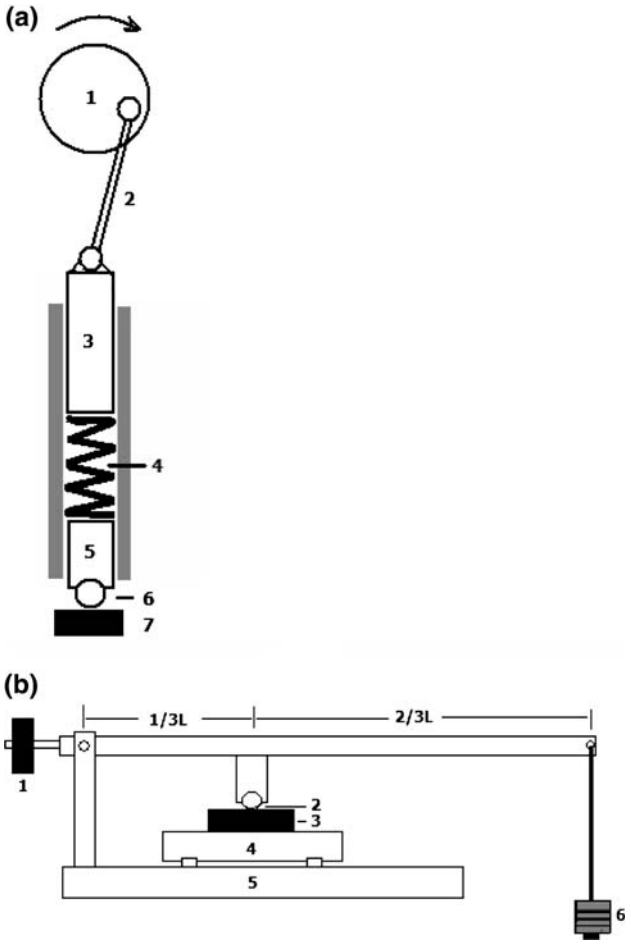

Fig. 1 Schematic diagram of test apparatus. (**a**) Test rig; (1) eccentric shaft, (2) loading arm, (3) upper slider, (4) spring, (5) lower slider, (6) ball, (7) PMMA plate. (**b**) Reciprocal friction test rig; (1) counter weight, (2) ball, (3) PMMA plate, (4) Sliding base, (5) table, (6) weight

Testing programme

All tests were conducted under dry contact conditions and at laboratory normal temperature. Cyclic load applied to the contact had mean value of 80 N and amplitude equal to 40 N. The same load conditions were used for all combination of materials in contact. The frequency of cyclic loading was 10 Hz. Figure 2 shows corresponding nominal maximum contact stress, calculated according to Hertz's equation for point contact, for the combination of materials in contact used.

For each combination of materials two identical tests were carried out to check repetitiveness of results. A third test was conducted if the two previous tests produced significantly different results. The test was interrupted at regular, predetermined time intervals, i.e. 5, 15, 30, 60, 180 and 810 min for examination of the surface damage development. Both PMMA plate and the

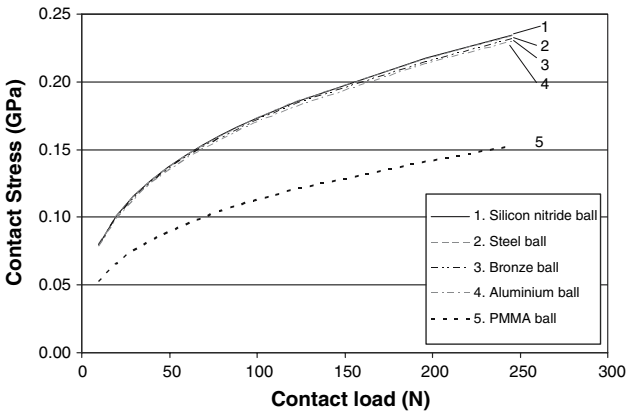

Fig. 2 The relationships between contact stress and contact load on the PMMA plate compressed against five types of ball

interacting ball were examined with optical microscope (OM) and scanning electron microscope (SEM). Energy dispersive X-ray (EDX) was used for investigation of material transfer between contacting surfaces. Profile of the wear scar formed on PMMA plate was reproduced with the help of Talysurf apparatus.

Results and discussion

In this section, test results obtained for each combination of materials used are discussed in turn in order to clearly identify the influence of the counterface material and the number of load cycles on the surface damage of PMMA.

For every combination of contacting materials, except Si_3N_4/PMMA, the occurrence of damage on PMMA surface was observed to happen during the first 5 min of testing under loading conditions specified earlier. Figure 3 shows damage features within the contact between PMMA plate and balls made of different materials produced after 5 min (equivalent to 3,000 load cycles). In Fig. 3, damage features within the contact of PMMA and Si_3N_4 ball were

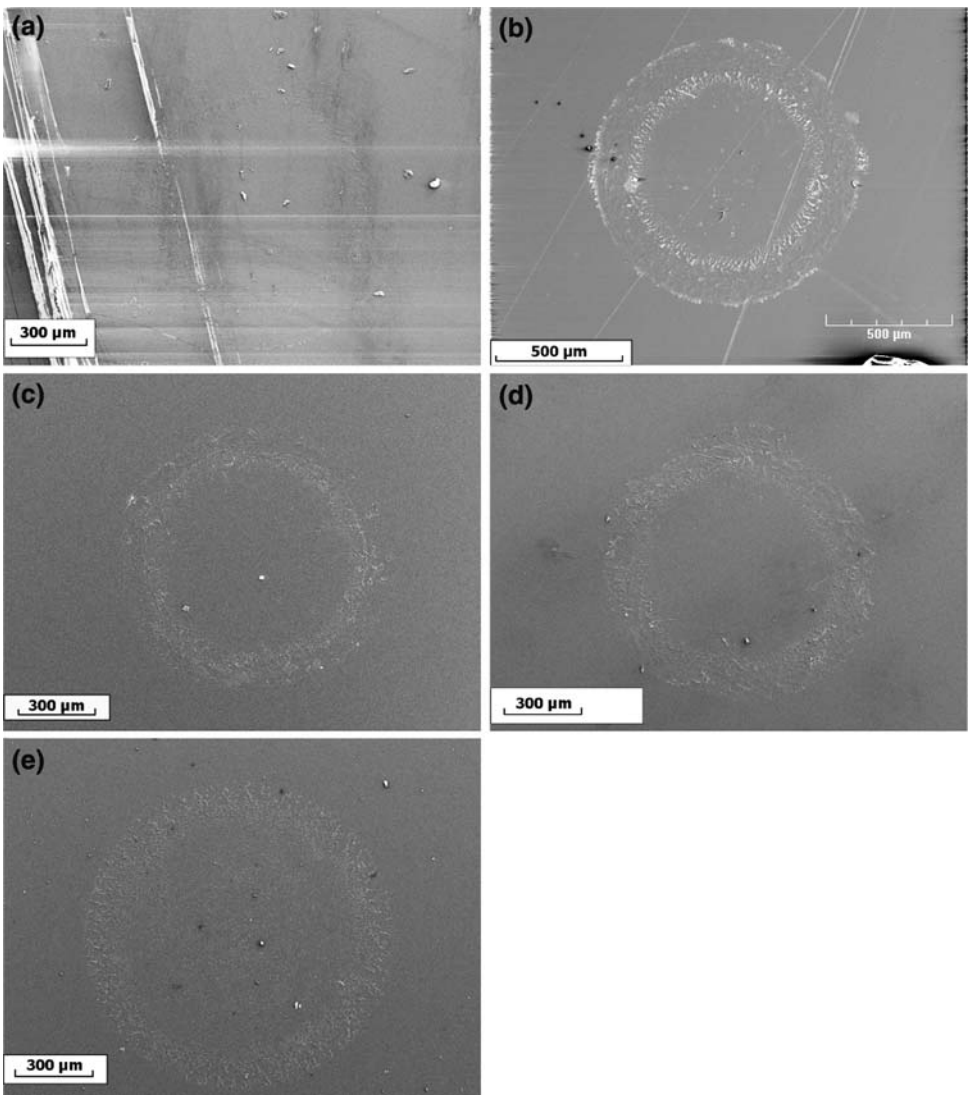

Fig. 3 SEM micrographs of PMMA plated tested against different ball. (**a**) Si_3N_4 ball 15 min, (**b**) steel ball 5 min, (**c**) aluminium ball 5 min, (**d**) bronze ball 5 min and (**e**) PMMA ball 5 min

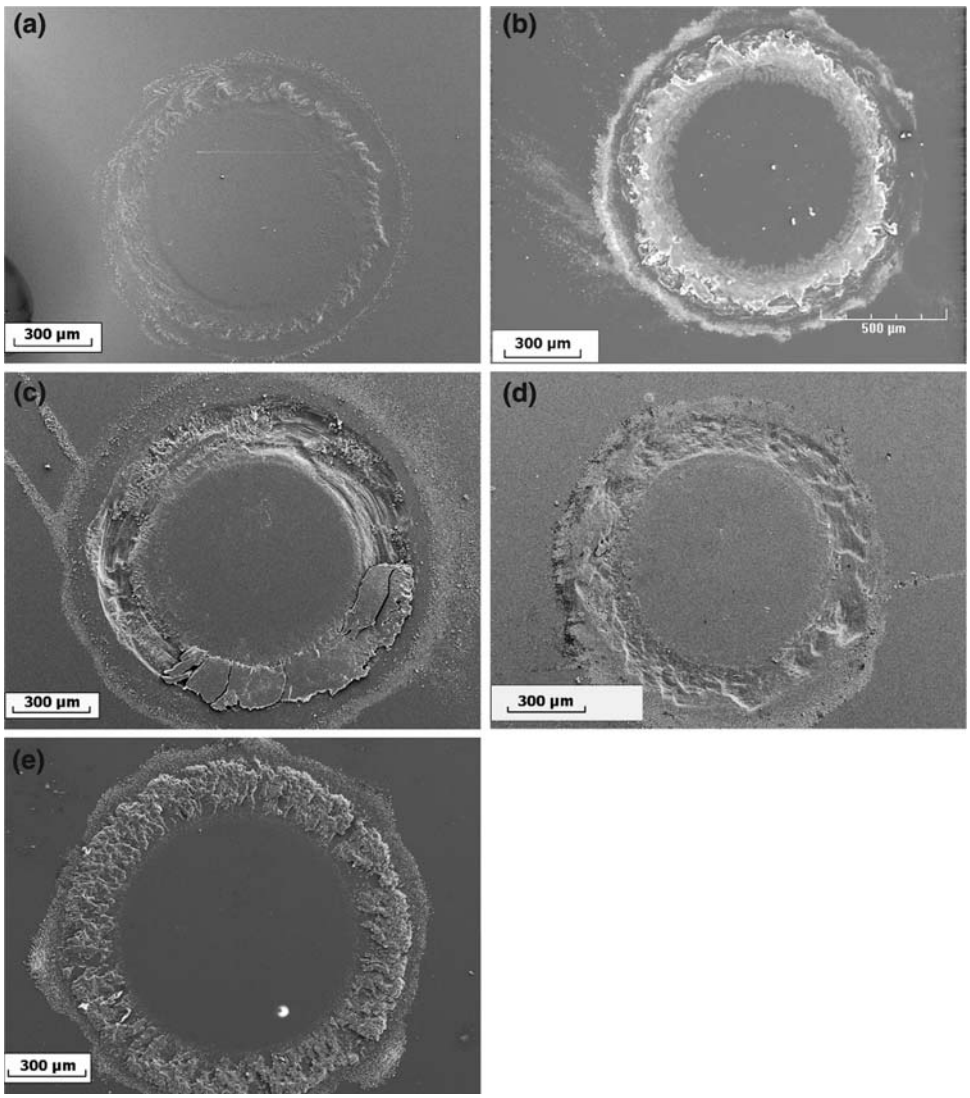

Fig. 4 SEM micrographs of PMMA plate test against different balls after test time 810 min. (**a**) Si_3N_4 ball, (**b**) steel ball, (**c**) aluminium ball, (**d**) bronze ball and (**e**) PMMA ball

produced after 15 min of testing (9,300 cycles). Figure 4 shows SEM micrographs illustrating damage features produced after 810 min (486,000 load cycles). In all cases, two regions within the contact area can be identified, namely stick region and slip region. It can be seen that the severe damage occurred in the slip region for all contact material combinations.

Si_3N_4/PMMA combination

Damage inflicted on PMMA plate during 5 min of testing is negligible. After 15 min of testing, the surface of PMMA plate was roughened especially around the stick region (see Fig. 3(a)). Wear debris produced were deposited in the vicinity of the contact circumference. After 30 min of testing, the surface roughness significantly increased within the slip region (see Fig. 5(a)). However, between 30 and 180 min of testing the contact area was not changed in any dramatic way.

Radial cracks were formed in the middle of the slip region after 810 min of testing (see Figs. 4(a) and 5(b)). Also, the surface roughness in the slip region increased and PMMA was transferred onto the ball surface (see Fig. 6).

Steel/PMMA combination

For this combination of contacting materials, the slip region became distinctly rough after only 5 min of testing (see Fig. 3(b)). Also, a small quantity of wear debris was produced and deposited at the edge of contact. After examination under SEM it was found that debris had flake-like shape. The general appearance of the contact region pointed the displacement of material and piling it up at the periphery of the contact area. Signs of melting of PMMA were quite evident as can be clearly seen near the boundary between stick and slip regions ripples (see Fig. 7(a)).

After 15 min of testing, the surface in the slip region increased its roughness and more wear debris were

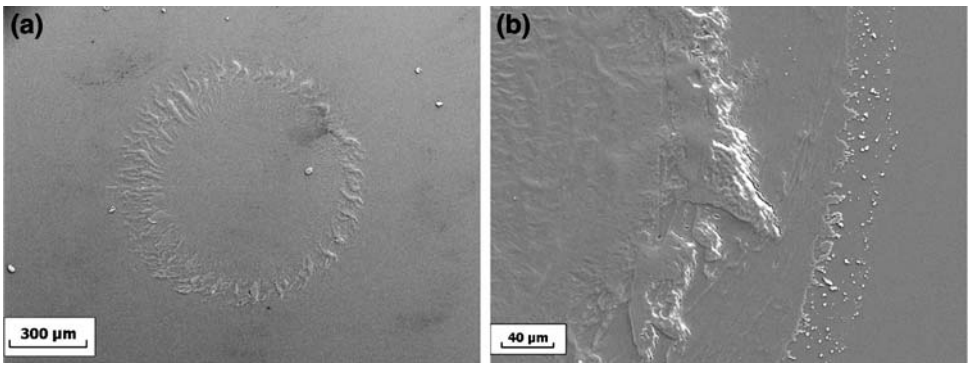

Fig. 5 SEM micrographs of PMMA plate tested against Si_3N_4 Ball; (**a**) test time 30 min and (**b**) test time 810 min

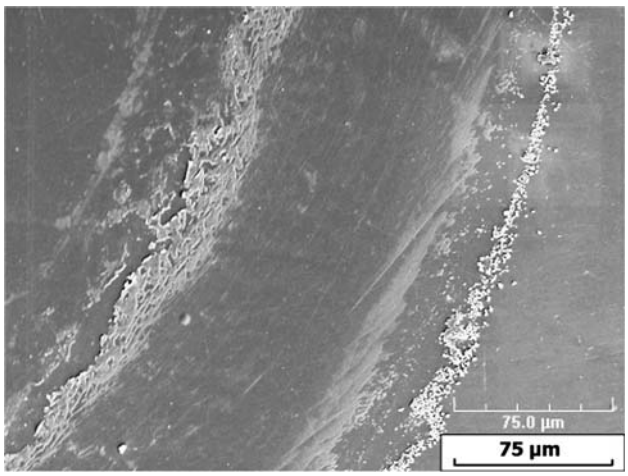

Fig. 6 SEM micrograph of Si_3N_4 ball surface shows transferred PMMA to the surface of the ball at the slip region

generated and deposited at the edge of the contact area. Surface micro-cracks appeared around the boundary of the stick region (see Fig. 7(b)).

Examinations under optical microscope clearly revealed that a ring-shaped zone composed of iron was formed at the boundary of the stick region after 60 min of testing (see Fig. 7(c)). In reflection mode this zone appeared shiny but in transparent mode it acquired a dark brownish colour. The iron-rich zone expanded outward with the increase in testing time. After 180 min of testing, lumps of detached material appeared in the slip region and abundance of wear debris accumulated at the edge of the contact area.

After 810 min of testing, ring cracks were formed along the edge of contact area (see Figs. 4(b) and 8). They appear to be initiated at the surface and grew into the bulk of PMMA plate. Propagation of cracks in the inward direction was clearly observed under optical microscope at higher

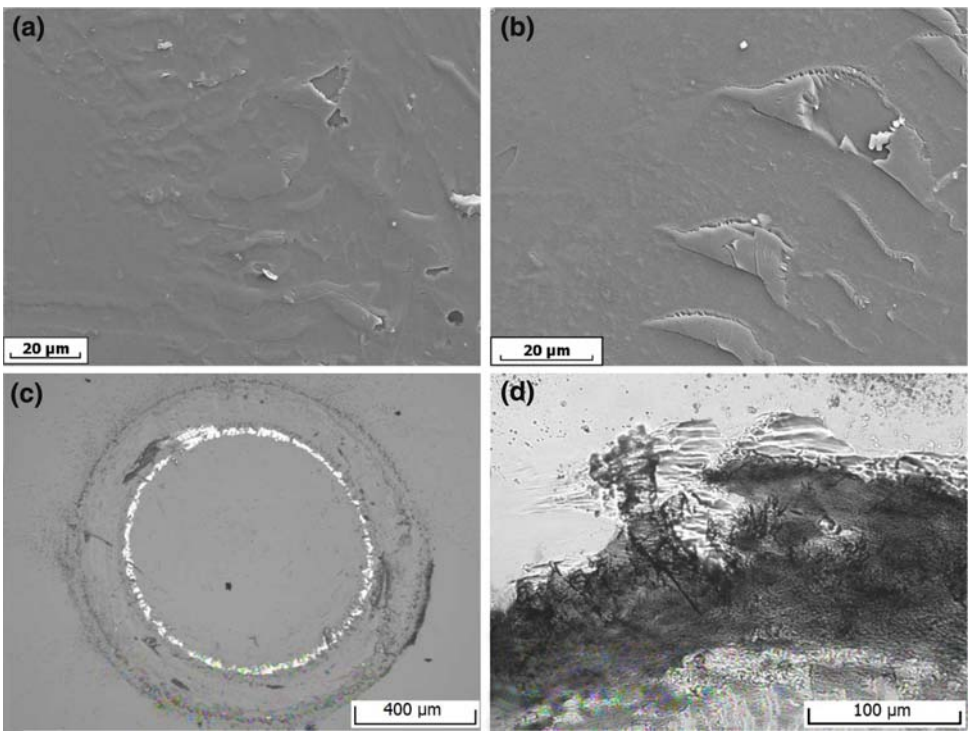

Fig. 7 (**a**, **b**) SEM micrographs of PMMA plate tested against steel ball. (**a**) High magnification at slip area, test time 5 min. (**b**) High magnification at boundary of slip area, test time 15 min. (**c**, **d**) Optical micrographs of PMMA plate. (**c**) Bright ring of iron rich region at the edge of stick boundary, test time 60 min. Picture was taken in reflection mode. (**d**) Cracks started at the edge of slip region and propagated deep down and inward to the stick boundary. Picture was taken in transparency mode. The dark colour of this area is because of iron compound transfer

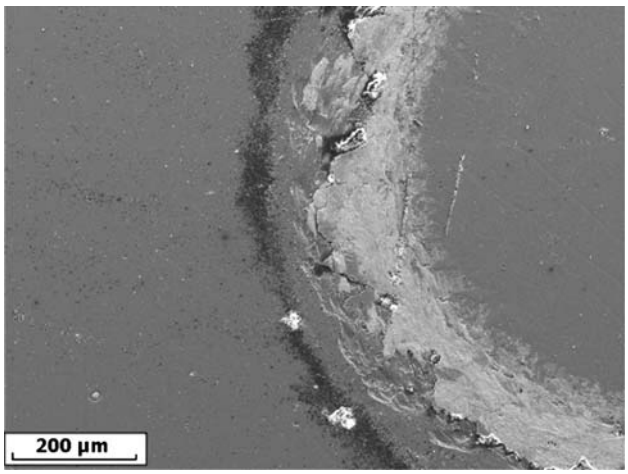

Fig. 8 SEM micrograph of PMMA surface shows ring cracks around the edge of slip region

magnification and transparent mode (see Fig. 7(d)). Also, copious quantity of wear debris was produced and deposited in the vicinity of the contact edge.

Aluminium/PMMA combination

Cracks were produced and transfer of material in the form of a thin film took place at the edge of the slip region after 5 min of testing (Fig. 3(c)). In reflection mode, bright, shiny fine particles could be seen under optical microscope (see Fig. 9(a)). The same particles appeared to be of a dark colour in the transparent mode (see Fig. 9(b)). EDX analyses confirmed that these particles were aluminium.

As the test duration was increased to 15 min, transfer of PMMA film continued and was mainly concentrated on the rim of the contact. However, only small amount of wear debris was produced and, as shown in Fig. 9(c), tiny white particles continued to be deposited at the boundary of the stick region. Also, in transparent mode, subsurface cracks could be seen when the test duration was extended to 30 min.

After 60 min of testing, cracks were found all over the slip region. Subsurface cracks could also be identified in the transparent mode (see Fig. 9(d)). A typical crack was initiated near the edge of the contact area and propagated into the bulk of the material in the direction of the boundary between the stick and slip regions.

After 810 min of testing, PMMA surface suffered heavy damage and sizeable pieces of material were either removed or loosely attached to the surface as evidenced by Fig. 4(c). Also, PMMA was transferred onto aluminium (see Fig. 10). The remaining of the contact area was covered by radial and circumferential cracks. Circumferential cracks were usually initiated at the edge of the contact area and propagated into the bulk of material and inward direction. At the boundary of the stick region, cracks emerged onto the surface.

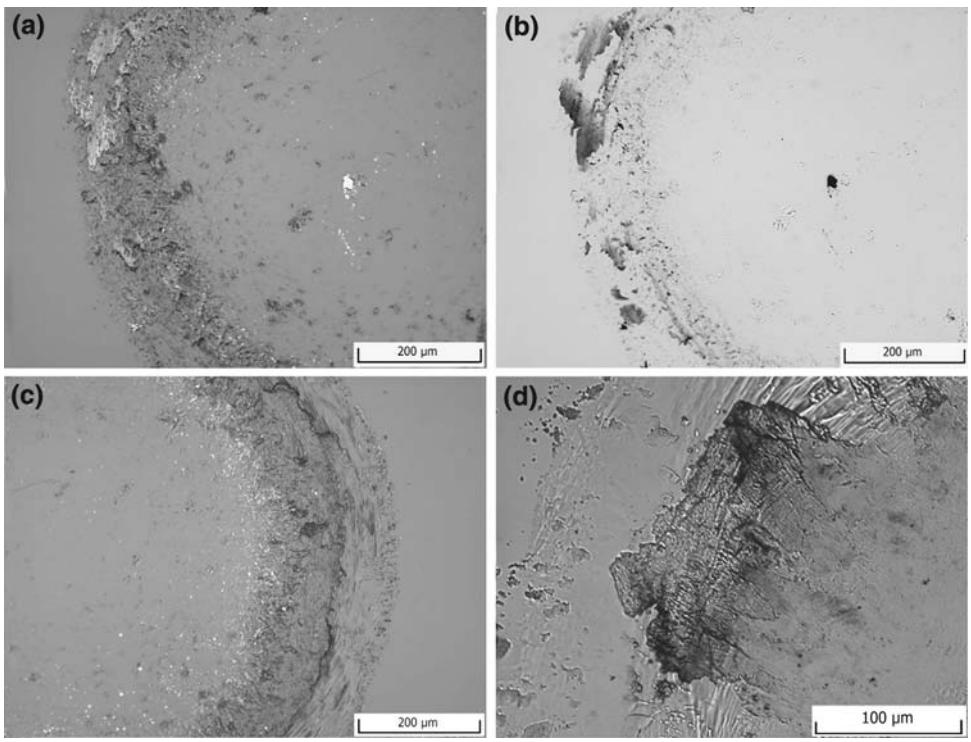

Fig. 9 Optical micrographs of PMMA plate test against aluminium ball. (**a**) Test time 5 min; surface roughened at the slip region and deposition of aluminium particles in both slip and stick region. Picture was taken in reflection mode. (**b**) The same position as (**a**), but photographed in transparency mode. The dark area shows aluminium rich region. (**c**) Test time 15 min; an intensely deposition of aluminium particles at the boundary region of stick area. Material loss was high at the edge of slip region. Photograph was taken in reflection mode. (**d**) Test time 60 min; cracks started from the edge of slip region and propagated deep down and inward to the boundary of the stick region. Photograph was taken in transparency mode

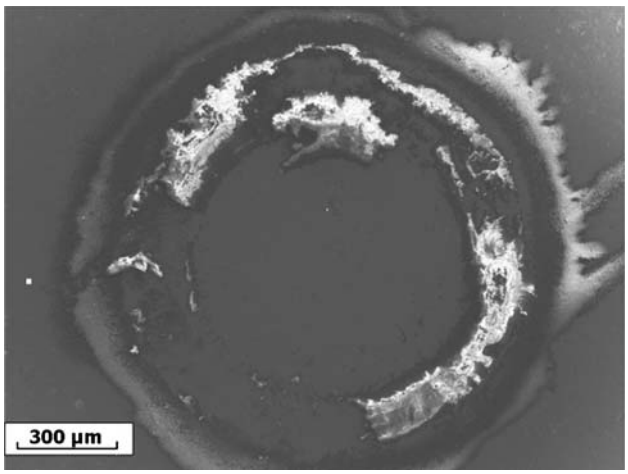

Fig. 10 SEM micrograph of aluminium ball surface shows transferred material to the surface of the ball at the slip region

Bronze/PMMA combination

In case of this combination of materials, 5 min of testing did not produce any noticeable wear. However, surface roughening took place in both stick and slip regions, although the slip region was slightly rougher (see Fig. 3(d)). Also, some transfer of the bronze took place as bright, yellowish fine particles embedded into the PMMA surface were observed (see Fig. 11(a)).

After 15 min of testing, ripples in the slip region appeared and more bronze particles were deposited in both slip and stick regions; however, deposition was especially noticeable at the rim of the slip region. Wear debris were produced and accumulated mainly at the periphery of the contact. Increasing testing time to 30 min did not produce any new features of surface damage.

After 60 min, a significant detachment of PMMA particles from within the slip region took place. Fine radial cracks were observed in transparent mode (see Fig. 11(b)). Surface damage intensified as testing time was increased to 180 min.

Volume loss of material in the form of sizeable fragments was observed in almost entire slip region after 810 min of testing (see Fig. 4(d)). Massive amount of wear debris was produced and deposited along the periphery of the contact. However, the stick region suffered relatively little damage.

PMMA/PMMA combination

When two identical materials were in contact, transfer from the ball onto the plate took place within the first 5 min of testing (see Figs. 3(e) and 12(a)). During that test interval transfer in opposite direction, that is from the plate onto the ball was not observed. Also, no wear debris was produced during 5 min of testing (see Fig. 12(a)).

Deposition of material on the plate, resulting from transfer from the ball, increased with the increase in testing time. The surface of the plate became progressively rougher. Also, wear debris began accumulating at the edge of the contact.

Transfer of material from the ball to the plate continued till the testing time reached 180 min (see Fig. 12(b)). However, the damage inflicted on the plate was quite severe compared to the damage suffered by the ball. During 180 min of testing, loose particles detached from the ball were transferred onto the plate as lumps. In transparent mode some radial cracks, hidden under transferred material, could be seen (see Fig. 12(c)). These cracks might be produced by expansion and contraction of the ball and the plate in circumferential direction during cyclic loading/unloading.

After continuous testing for 810 h, material from the ball transferred to the plate was covering almost entire slip region (see Fig. 4(e)). Most severe wear of the ball was located on the outermost region of the contact annulus. Also, the damage inflicted on the ball was far more extensive than that suffered by the plate.

Discussion of results

In summary, PMMA plate showed significantly different degrees of damage when in dry contact with different

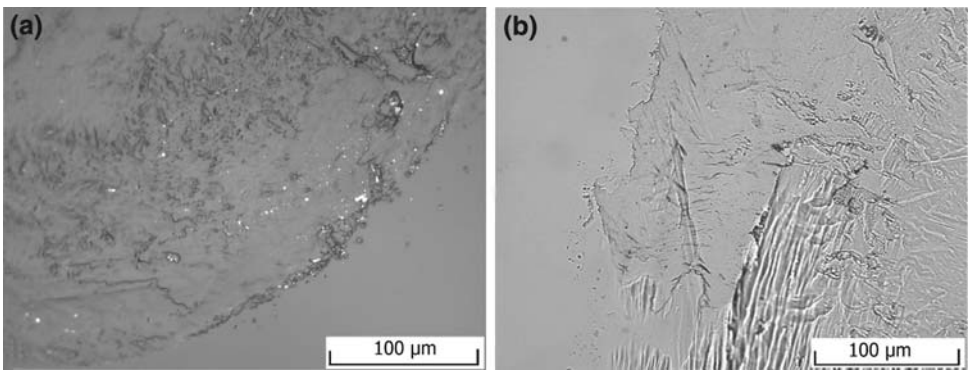

Fig. 11 Optical micrographs of PMMA plate tested against bronze ball. (**a**) Test time 5 min; tiny particles of bronze deposited at the contact area specially the edge of slip region. Surface at slip region was roughened. Picture was taken in reflection mode. (**b**) Test time 60 min; detachment of PMMA surface and fine radial cracks were found in some area in the slip area

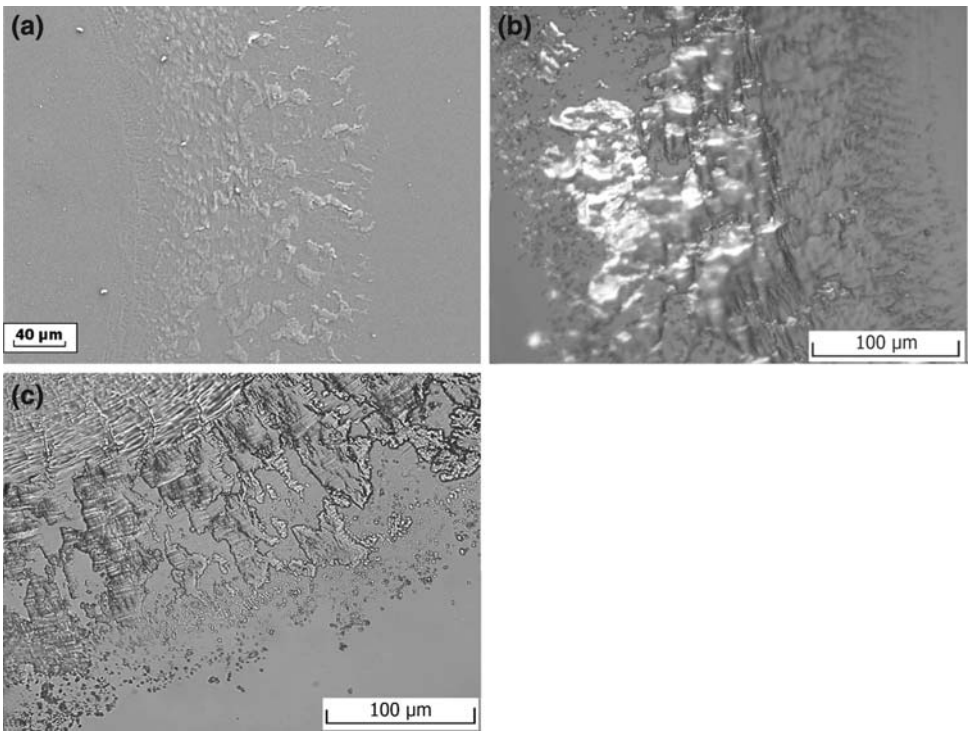

Fig. 12 SEM micrograph (**a**) and optical micrographs (**b**, **c**) of PMMA plate tested against PMMA ball. (**a**) Test time 5 min; material transferred form PMMA ball. (**b**) Test time 60 min; material was lost from PMMA plate at the area next to the stick boundary region. Photograph was taken in reflection mode. (**c**) The same sample as (**b**), but different position. Radial cracks were observed in the deposits of lump transferred material from the ball. The photograph was taken in transparency mode

couterface materials. Under load conditions applied, contact with silicon nitride ball resulted in shallow microcracks. Contact with steel, aluminium and bronze balls produced ring-shaped microcracks located in the slip region. Cracks were initiated at the edge of the slip region and propagated into the bulk of the material. When they had grown half way through the slip region, they started to emerge and reached the surface in the vicinity of the stick region's boundary especially in case contact with aluminium ball.

According to the Hertz's equation for point contact, the PMMA plate was subjected to varying contact stress. The level of contact stress can be ranked as follows: the highest was for silicon nitride, then it decreased for steel, bronze and aluminium, reaching the lowest level for PMMA ball. This ranking is illustrated in Fig. 2. However, the least damage of the PMMA plate was observed when it was in contact with silicon nitride ball (highest contact stress). On the other hand, for the lowest contact stress used during this study (PMMA/PMMA combination), damage suffered by the plate was rather minor but the ball's damage was quite severe. This clearly implies that the level of applied contact stress is not the only factor governing the damage inflicted on the PMMA plate.

The crack pattern observed by many other researchers is the form of ring cone cracks. It is known that the formation of ring cone cracks is influenced by tensile stress, which occurs maximum just next to the edge of contact. In this study it was found that the damage morphology is different than that normally expected and observed. Cracks were initiated in the outer zone of the slip annulus and propagated inward to the boundary between the slip and stick region.

In general, there are three factors affecting the contact between materials: stress level, friction and affinity to form adhesive junctions. If only contact stress is considered then it is apparent that the highest stress applied to the PMMA plate resulted from its contact with silicon nitride ball; hence, damage ought to be most severe but that was not the case. Similarly, damage suffered by the PMMA plate ought to be the least when in contact with aluminium ball (second lowest contact stress applied) but again that was not the case. Clearly, either friction and adhesion or both must govern the extent of damage inflicted on the PMMA plate.

Accordingly, friction measurements were carried out to ascertain the level of friction force characteristic for all material combinations studies. Adhesion is another phenomenon taking place when materials are in an intimate, close contact and is manifested by the formation of adhesive junctions and junction growth. However, it was clearly observed that tiny metallic particles were firmly attached to the PMMA surface. This infers occurrence of strong adhesion and shearing of junctions at the slip region's interface. It was practically impossible to measure adhesion at the points of real contact; however, indirect evidence of adhesion might be provided by the results of EDX measurements.

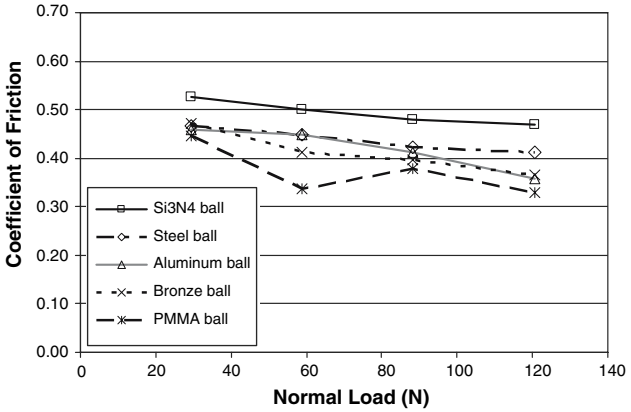

Fig. 13 Relationships between coefficient of friction and normal load of PMMA tested against different balls

Results of auxiliary experiments and measurements

Results of friction experiments

Friction measurements for all combinations of materials used in surface fatigue tests were carried out. Test apparatus, schematically shown in Fig. 1(b), was used. Tests were conducted with the load on the contact depending on the combination of materials. The load increased step-wise until it reached the magnitude comparable with the load applied on the contact during surface fatigue tests. The friction coefficient as a function of normal load on the contact was plotted and is shown in Fig. 13.

The first observation is that friction coefficient has a tendency to decrease with increasing contact load. This agrees well with experimental results reported by others [11]. Coefficient of friction for the Si_3N_4/PMMA pair was found to be the highest while for the PMMA/PMMA pair the friction coefficient was lowest and that is true for the entire load range used. For example, at the contact load of 30 N, the ranking of materials in frictional contact with PMMA plate from the highest to lowest value of the friction coefficient is as follows: silicon nitride, bronze, steel, aluminium and PMMA, respectively. The only exception from that was observed at the contact load of 120 N where friction coefficient for bronze was lower than that for steel.

The magnitude of friction within the contact provides indication of the shear stress at the contact interface. However, there is no obvious correlation between the magnitude of friction/shear stress and the severity of damage as the Si_3N_4/PMMA contact with highest friction suffered the least damage. It means that the shear stress at the contact interface, as manifested by the level of friction, does not seriously affect the extent of damage inflicted on a static contact subjected to a cyclic normal load.

Results of energy dispersive analyses

In order to confirm the adhesion between the PMMA plate and counterfaces used, EDX technique was used. Figure 14 shows a typical output form EDX analysis for the steel/PMMA contact. It is seen that iron and oxygen were detected in the slip region of the contact. This confirms that material from the steel ball was transferred onto the surface of PMMA plate. The results of element mapping are shown in Fig. 15. The transfer of iron from the steel ball is presumably the result of adhesion and slipping within the slip region of the contact. EDX results for other contact pairs confirm that adhesion took place but to a different extent. The Si_3N_4/PMMA contact proved to have the least propensity to form adhesive junctions and subsequent transfer of material.

Results of surface profile measurements

Profiles of the contact scar were generated at the end of each test interval in order to monitor the development of

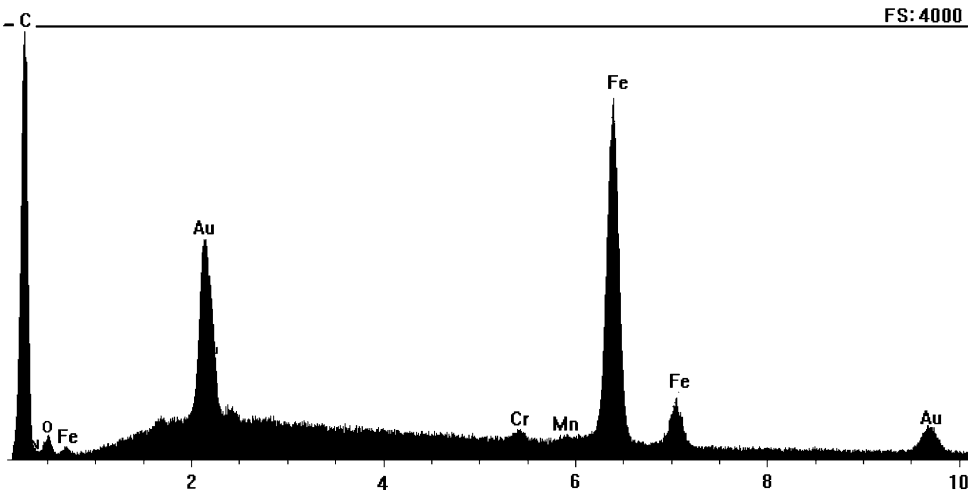

Fig. 14 EDX analysis results show chemical compositions at the slip area of the surface of PMMA plate tested against steel ball for 810 min. The results show high portion of iron and amount of oxygen. Gold (Au) is from surface coating for electrical conducting purpose because PMMA is non-conductive material

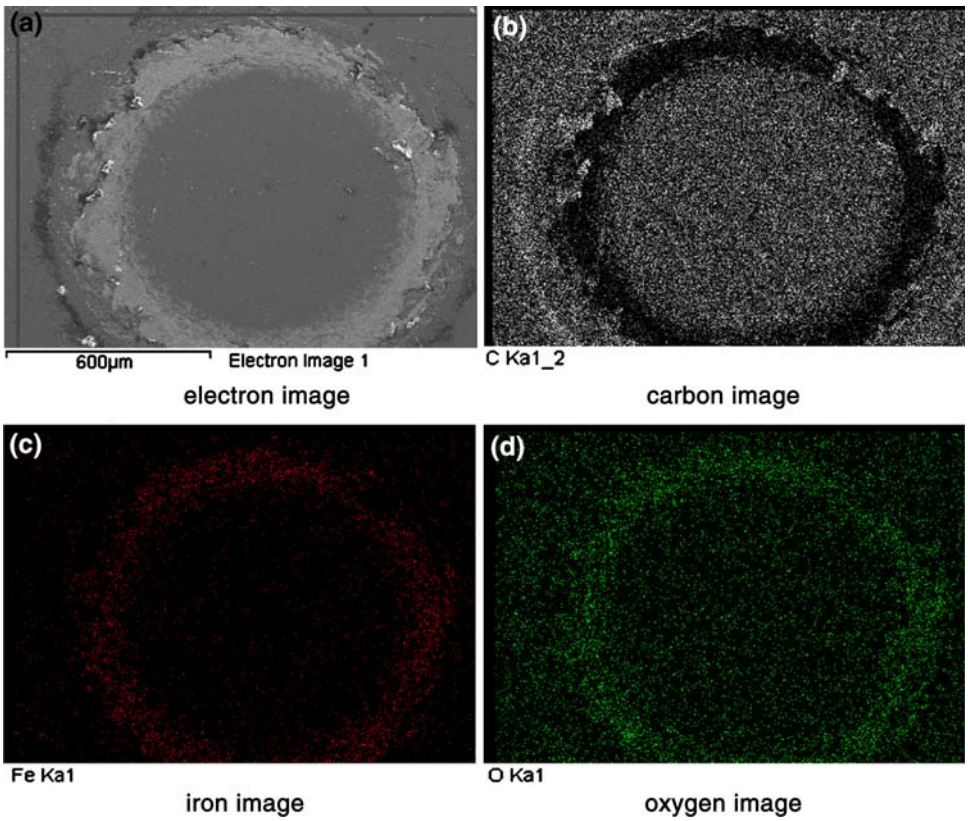

Fig. 15 Mapping images of PMMA plate at contact area tested against steel ball for 810 min show rich of iron and oxygen in slip region

contact signature on PMMA plate. Figure 16 shows profiles for all contact pairs investigated after 810 min of testing. It can be inferred from these profiles that the damage is mainly concentrated within the slip region of the contact. The deepest scar was recorded for bronze/PMMA pair and the shallowest for the PMMA/PMMA pair. Aluminium, steel and silicon nitride counterfaces produced scars with descending depth, respectively. Pilling up of the material within the slip region should be noted. This provides indirect evidence that adhesion of PMMA to the counterface took place. During unloading of the contact, due to elastic recovery, some movement at the contact interface takes place. If the strength of interface within the slip region is greater than that of bulk PMMA, then the material will be strained causing transfer and initiating cracks in the plate. In case of PMMA/PMMA contact, cracks were observed to occur on the surface of the PMMA ball, which can be taken as an indication of greater strain imposed on the ball in contact with a nominally flat surface.

Conclusions

Damage of the PMMA plate under cyclic normal load imposed its dry contact with a ball made of five different materials depends on a number of parameters as revealed by the results. The main findings can be summarised as follows:

1. Material of the counterface plays an important role in the damage process of PMMA. It was found that the least damage of the PMMA plate resulted from its contact with silicon nitride ball. Contact with steel, aluminium and bronze balls, respectively, produced damage in ascending order of severity.
2. The predominant form of damage suffered by the PMMA plate consisted in ring cracks leading to substantial wear. It is reasonable to say that cracks were initiated during the unloading cycle and the creation was influenced by the material of the counterface.
3. Cracks were usually created in the slip region of the contact and in close vicinity to its boundary with the stick region when PMMA plate was in contact with silicon nitride ball. When the contact was with steel, bronze and aluminium balls, cracks were initiated at the outer edge of the slip region.
4. Adhesion and creation of adhesive junctions within the contact between the PMMA plate and balls made of different materials appear to be the key factors for crack initiation and damage.

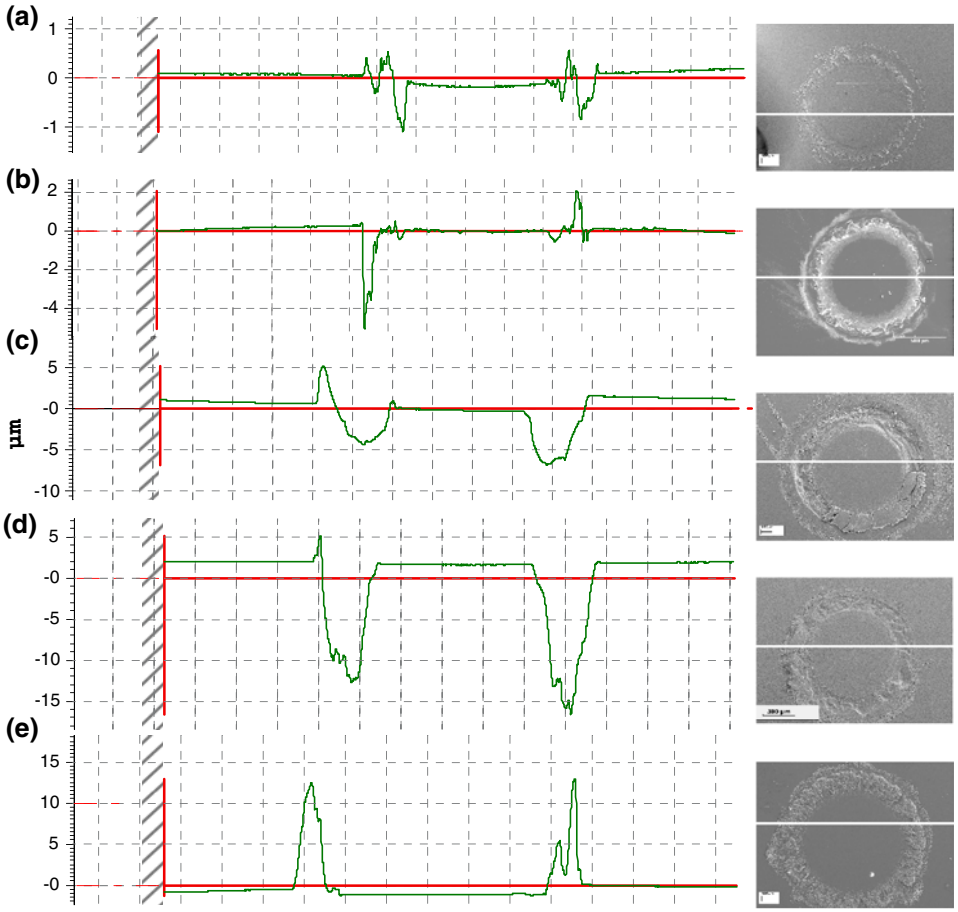

Fig. 16 Profile measurements of PMMA plate tested against different balls after 810 min. (**a**) Si_3N_4 ball, (**b**) steel ball, (**c**) aluminium ball, (**d**) bronze ball and (**e**) PMMA ball. Measurements conducted along the white line on the right hand side

5. The PMMA plate did not suffer any substantial damage when in contact with PMMA ball. Instead, the ball was damaged much more substantially.
6. Transfer of material between contacting surfaces took place but to a different extent depending on the type of conterface material.

References

1. Alfredsson B, Olsson M (2000) Eng Frac Mech 65:89
2. Eyzop BL, Karlsson S (1999) Wear 225–229:1303
3. Chen Z, Cuneo JC, Mecholsky JJ, Hu S (1996) Wear 198:197
4. Kim DR, Jung Y-G, Peterson IM, Lawn BR (1999) Acta Mater 47:4711
5. Zhu MH, Zhou ZR, Kapsa Ph, Vincent L (2001) Wear 250:650
6. Johnson KL (1985) Contact mechanics. Cambridge University Press, p 62
7. Guiberteau F, Padture NP, Cai H, Lawn BR (1993) Philos Mag A 68:1003
8. Zhu MH, Yu HY, Zhou ZR (2006) Tribol Int 39:1255
9. Fouvry S, Fridrici V, Langlade C, Kapsa Ph, Vincent L (2006) Tribol Int 39:1005
10. Briscoe BJ, Chateauminois A, Lindley TC, Parsonage D (1998) Tribol Int 31:701
11. Archard JF (1957) Proc R Soc Lond A 243:190